Wasit Journal of Engineering Sciences
Journal homepage: https://ejuow.uowasit.edu.iq
Vol. 14 No. 2 June 2026, pp.91-100
https://doi.org/10.31185/ejuow.v14i2.774

ISSN 2305-6932
Original Research

Performance Comparison of DFT and RDFT Systems Based on Optical-OFDM in PAPR Reduction

Ameen S. Jasim[1], Mounir T. Hamood[1]
[1] Department of Electrical Engineering, College of Engineer, Tikrit University, Tikrit, Iraq

Corresponding Author Email: as230042en@st.tu.edu.iq

Received Aug.5, 2025 Revised Sept.28, 2025 Accepted Oct.6, 2025 Online Jun.1, 2026

ABSTRACT

This study investigates an advanced Visible Light Communication (VLC) system employing Real Discrete Fourier Transform (RDFT)-based DC-biased Optical OFDM (DCO-OFDM), focusing specifically on the reduction of Peak-to-Average Power Ratio (PAPR) via the Walsh-Hadamard Transform (WHT). This study aims to reduce the substantial computational complexity and power inefficiency of traditional DFT-based DCO-OFDM systems, while preserving comparable Bit Error Rate (BER) performance. The RDFT is a superior mathematical approach compared to the DFT as it eliminates the need for costly Hermitian symmetry calculations. This reduces the quantity of real multiplications and real additions by 50%. The system has been simulated in MATLAB using N=256 over an Additive White Gaussian Noise (AWGN) channel, employing 16-ary Phase-Shift Keying (16-PSK) and 16-ary Quadrature Amplitude Modulation (16-QAM) modulation techniques. The results demonstrate that DCO-OFDM with RDFT shows a BER performance akin to that of DFT-based systems. At an SNR of approximately 33.5 dB, 16-PSK has a BER of 10^{-4}. At an SNR of approximately 29.5 dB, 16-QAM exhibits an equivalent BER. The application of WHT pre-coding reduces PAPR; for example, RDFT-WHT demonstrates a decrease of approximately 0.5 dB at a CCDF of 10^{-4} compared to the exclusive use of RDFT. Upon examining complexity, it is evident that both addition and multiplication have been simplified. The findings indicate that the RDFT-WHT-based system is the optimal choice for future optical wireless communication systems due to its user-friendliness, energy efficiency, and superior performance compared to alternative systems.

Keywords: BER, DCO-OFDM, DFT, PAPR, RDFT, WHT

1. Introduction

Visible Light Communication (VLC) encompasses modulation techniques that can be categorized into single-carrier modulation (SCM) and multi-carrier modulation (MCM). SCM techniques, including analog pulse modulation and on-off keying (OOK), are employed in VLC systems, which can lead to low data rates. MCM techniques, including O-OFDM, have been introduced to address this limitation [1]. However, the fundamental principle in VLC systems is IM/DD, which means that optical OFDM (O-OFDM) is also constrained by the necessity for a real, non-negative signal in the time domain [2]. Among O-OFDM schemes, Direct Current-biased Optical OFDM (DCO-OFDM) and Asymmetrically Clipped Optical OFDM (ACO-OFDM) are commonly used. DCO-OFDM supports the transmission of all subcarriers, enabling higher spectral efficiency than ACO-OFDM, which uses only odd subcarriers and discards the rest to maintain signal non-negativity. Although DCO-OFDM requires a DC bias, which leads to reduced power efficiency, it offers greater flexibility and throughput, making it more suitable for high-data-rate applications [2, 3]. Conventional methods utilize the inverse DFT (IDFT) for the implementation of OFDM, exemplified by DCO-OFDM [4]. However, these methods incur significant computational expenses [5]. Various alternative transforms, including RDFT, have been examined to address these issues. RDFT offers several advantages, including straightforward computation

and rapid processing. O-OFDM utilizing RDFT maintains the necessary Hermitian symmetry to produce a genuine IM/DD waveform. The efficiency arises from the integration of positive-frequency components, both real and imaginary, while allowing the real-data transformation to manage the conjugate mirror independently. RDFT-based O-OFDM systems exhibit equivalent spectral efficiency to DFT-based systems, reduced power consumption, and straightforward setup and usability. The findings indicate that the RDFT enhances the performance and efficiency of VLC systems relative to conventional DFT-based approaches. The increasing demand for rapid and secure communication systems highlights the importance of VLC systems, particularly DCO-OFDM, which utilizes advanced transforms such as RDFT, in the future of optical communication systems [6]. The proposed low-PAPR/low-complexity chain is appropriate for indoor Light-Fidelity (Li-Fi) access networks, areas with weak Radio Frequency (RF) signals such as hospitals and airports, interconnecting head and tail lights in vehicles, providing illumination for industrial Internet-of-Things (IoT), and facilitating secure short-range localization and communication in smart buildings. This paper is organized as follows: Section 1 presents an overview of visible light communication, outlining its benefits and the associated research problem. Section 2 discusses the DFT-based DCO-OFDM method and its computational complexity. Section 3 outlines the methodology employed to address the fixed issue by RDFT-based DCO-OFDM and the computational complexity of RDFT and discusses the Walsh-Hadamard transform, a technique used to minimize PAPR. Section 4 discusses the theoretical framework and simulation methods employed to address the problem. Section 5 presents the results obtained, while Section 6 provides the conclusion. The notation * represents complex conjugate, $\Re/\Im$ Real/Imaginary components, μ Proportionality Constant,$E\cdot$ Statistical Expectation.

2. Background and Related Work

Many individuals are intrigued by O-OFDM due to its potential application in rapid wireless communication. A prevalent variant of O-OFDM systems is DCO-OFDM. This occurs due to the utilization of all subcarriers, hence enhancing spectrum efficiency. The DFT is a conventional technique that requires substantial computational resources and exhibits a high PAPR, hence impeding system performance. Recent studies have explored alternative transforms, including the RDFT and the WHT, aimed at reducing complexity and the PAPR, resulting in significant improvements while maintaining BER performance.

2.1. DFT-based DCO-OFDM

For OFDM signals, the address frequencies $X(k)$ are minimally Hermitianized at the input of an N-IDFT block:

$$X(k) = X^*(N-k), \quad k = 1,2,\dots,\big((N/2)-1\big), \tag{1}$$

Where N represents the transmitter signal, and * indicates the associated direction. $X(0)$ and $X(N/2)$ should be assigned a value of zero [7]. As shown in Fig. 1, the serial input data after mapping is processed through the IDFT module to generate the discrete time-domain signal $x(n)$, which is defined as [8]:

$$x(n) = \frac{1}{N}\sum_{n=0}^{N-1} X(k)\exp\left(j2\pi\frac{nk}{N}\right), \tag{2}$$

$X(k)$ and $x(n)$ represent the structured transmitter in the frequency domain and the unipolar signal in the time domain, respectively.

The DC-bias value is estimated to be zero at the output of the IDFT, and all other bias values are subsequently clipped to zero. The DC-bias is expressed as a function of the elastic bias of $x(n)$ [8], as indicated in Eq. (3) and Eq. (4):

$$B_{\mathrm{DC}} = \mu\cdot E[s(t)^2], \tag{3}$$

$$x(n) = x(n) + B_{\mathrm{DC}}, \tag{4}$$

Where μ represents the proportionality constant and $E[\cdot]$ denotes the statistical expectation on the right side of the equation [9]. Typically, designers use a DC bias of 7 dB [7]. This fails to meet the transmitter requirements,

resulting in clipping that introduces noise in both the even and odd optical transmissions. Cyclic Prefix (CP) is incorporated into the OFDM symbols to address the issue of inter-symbol interference (ISI). The DCO-OFDM signal is transmitted through the optical channel, which is subject to Additive White Gaussian Noise (AWGN). The cyclic prefix (CP) and direct current (DC) component are eliminated at the receiver, followed by the application of the DFT. Next, the data subcarriers are selected and demapped using a demapper [7-9].

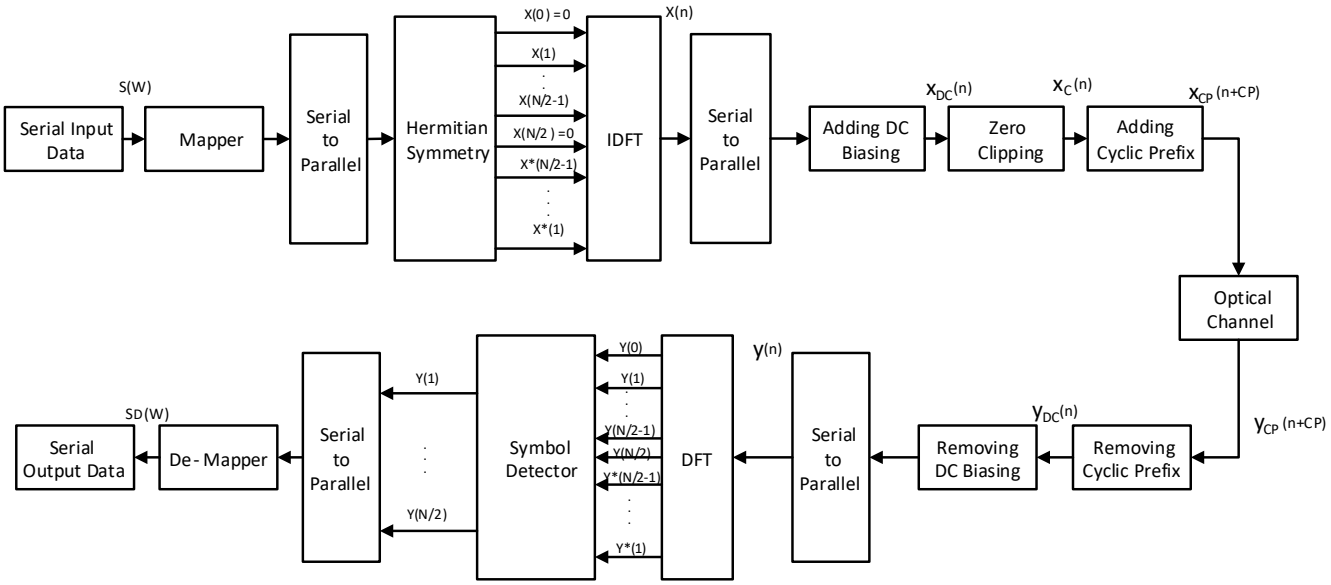

Figure 1. DFT-Based DCO-OFDM Block Diagram

2.2. Computational complexity of DFT

The DFT $O(N^2)$ operations are used to compute the real and imaginary components of a signal of length N. This indicates that the number of processes increases by a factor of four for each additional unit of input. To apply the DFT formula, it is necessary to determine N output frequency components, which requires the addition and multiplication of N complex numbers [10].

Each complex multiplication necessitates 4 real multiplications and 2 real additions. While 2 real additions are required for each complex addition. A total of $N(N-1)$ complex additions and N^2 complex multiplications are required. These operations could be converted into real operations by:

Total real multiplications of DFT (C_M):

$$C_M = 16N^2, \tag{5}$$

The cumulative count of real additions in the DFT (C_A) is expressed as:

$$C_A = 4N^2 - 2N, \tag{6}$$

3. Method

This study presents an RDFT-based framework enhanced with WHT pre-coding to address the drawbacks of conventional DFT-based DCO-OFDM for PAPR reduction. The RDFT does not require Hermitian symmetry, hence reducing the number of multiplications by fifty percent and simplifying the operation significantly. WHT enhances the system by decreasing PAPR through the reduction of data correlation prior to transmission. MATLAB simulations over an AWGN channel, along with modulation techniques for both 16-PSK and 16-QAM, were employed to evaluate the system and ensure its functionality. Critical characteristics, such as BER, PAPR, and computational complexity, were evaluated to determine if the proposed method exceeds existing DFT-based techniques.

3.1. RDFT-based DCO-OFDM

DCO-OFDM utilizes all available subcarriers to achieve a higher spectral efficiency. In order to produce the time domain signal where the complex modulated data symbols are denoted by $s(w)$, the correct conjugate

symmetry is ensured by the negative sign on the imaginary components. The modulated data symbols are arranged to maintain conjugate symmetry. The real/imaginary part of the complex modulated symbol is split and aligned at the correct positions in the frequency domain vector in order to ensure that the IRDFT output is real-valued [6], as shown in Fig. 2.

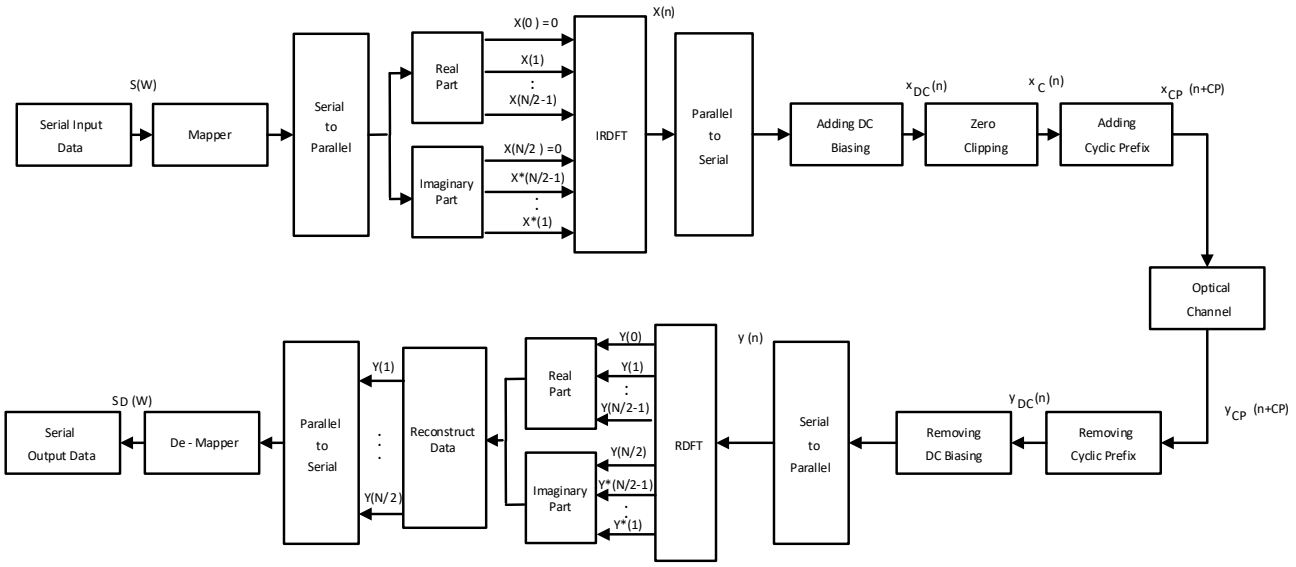

Figure 2. DFT-Based DCO-OFDM Block Diagram

The time domain signal is obtained through IRDFT processing:

$$x_{IRDFT}(n) = [0, \Re(s(1)), \Re(s(2)), \ldots, \Re(s(N/2-1))], [0, -\Im(s(N/2-1)), \ldots, -\Im(s(2)), -\Im(s(1))] \quad (7)$$

A consequence of using all subcarriers in DCO-OFDM is that the time-domain signal includes both positive and negative values. To make the signal compatible with IM in optical systems, a DC bias is used to shift the signal samples to positive values [1].

$$x_{DC}(n) = x_{IRDFT}(n) + B_{DC} \quad (8)$$

After the above truncation, the remaining negative samples due to inadequate bias or noise are truncated to zero. In optical transmission, a CP is added to avoid ISI. The receiver incorporates a photodiode for converting the optical signal from optical to electrical form after it has been transmitted through the IM/DD channel. The DC bias of the received signal is eliminated as a result of the cyclic prefix removal and analog-to-digital conversion [11]:

$$y(n) = x_{CP}(n + CP) - B_{DC} \quad (9)$$

Where $y(n)$ represents the received signal, which includes the DC bias. Subsequently, the signal is processed using RDFT and subsequently returned to the frequency domain. The frequency domain signal structure of the RDFT can be expressed as follows:

$$Y_{DCO} = [\Re(y(1)) - j\,\Im(y(N/2-1)), \Re(y(2)) - j\,\Im(y(N/2-2)), \ldots, \Re(y(N/2-1)) - j\,\Im(y(1))] \quad (10)$$

DCO-OFDM experiences clipping distortion across all subcarriers when insufficient DC bias is applied. Nevertheless, clipping can be mitigated by selecting the appropriate DC bias. The data symbols are effectively recovered after demodulation, and the original data stream is reconstructed through parallel-to-serial conversion. The primary advantage of RDFT-based DCO-OFDM over traditional DFT-based DCO-OFDM is the computational efficiency achieved through real-valued processing, which requires approximately half as many operations while maintaining full subcarrier utilization and spectral efficiency.

3.2. Computational complexity of RDFT

The RDFT utilizes the Hermitian symmetry inherent in real signals. It is necessary to identify $N/2 + 1$ within the frequency components. Each input sample in every component of the RDFT requires 2 real additions and 2 real multiplications [6, 12]. The total count of real multiplication operations in RDFT ($R_M(N)$) is:

$$R_M(N) = 8N^2, \tag{11}$$

The following equation represents the total count of real addition operations for RDFT ($R_A(N)$):

$$R_A(N) = 2N(N-1), \tag{12}$$

3.3. Walsh-Hadamard transform

The WHT significantly decreases PAPR in OFDM systems. The Hadamard Transform matrix (H) is a square matrix defined by elements that assume values of either 1 or -1, and it plays a crucial role in minimizing the autocorrelation of the input data sequence. The Hadamard matrix of order 2 is defined as follows:

$$H = \frac{1}{\sqrt{2}}\begin{bmatrix} 1 & 1 \\ 1 & -1 \end{bmatrix} \tag{13}$$

This method may decrease the number of signal peaks without necessitating further information from the receiver and produce symbol sequences with diminished correlation by aligning the order N of the Hadamard matrix with the number of OFDM subcarriers [13]. This enables more efficient management of power peaks. Prior to the application of the IDFT, pre-coding techniques improve the WHT by multiplying frequency-domain modulated data blocks with a designated pre-coding matrix H. In the absence of rate loss considerations, the dimensions of the pre-coding matrix are generally $N \times N$, signifying no penalties related to data rate [14]. Recent advancements in WHT-based pre-coding methods for O-OFDM systems focus on reducing PAPR by minimizing data autocorrelation. The structured Hadamard matrix enables this capability, while the recursive generation method guarantees the consistent production of low-correlation output signals, thereby significantly improving system performance [15].

4. Simulation

Performance analysis and simulations were conducted in an AWGN channel using MATLAB for this work. The system's parameters are set up in Table 1:

Table 1. System Parameters

Parameter	Symbol	Value
Number of Subcarriers	N	256
Cyclic Prefix Length	CP	N/4
DC-bias	B_{DC}	7 dB
Modulation Order	M	16
OFDM symbols for BER	$Symbols$	10^4
OFDM symbols for PAPR	$Symbols$	10^5
Signal-to-Noise Ratio	SNR	45 dB
Channel	$AWGN\ Channel$	AWGN

We examined trade-offs dependent on the constellation while maintaining spectral efficiency by employing both 16-PSK and 16-QAM (4 bits/symbol each): The constant-modulus symbols of PSK can enhance the linearity of the front end; nevertheless, they often require a higher Eb/N0 to achieve the same BER as QAM. QAM

consumes less power; yet, its amplitude exhibits greater fluctuations. The flow chart for utilizing RDFT and WHT with DCO-OFDM, as well as calculating BER and PAPR performance, is shown in Fig. 3.

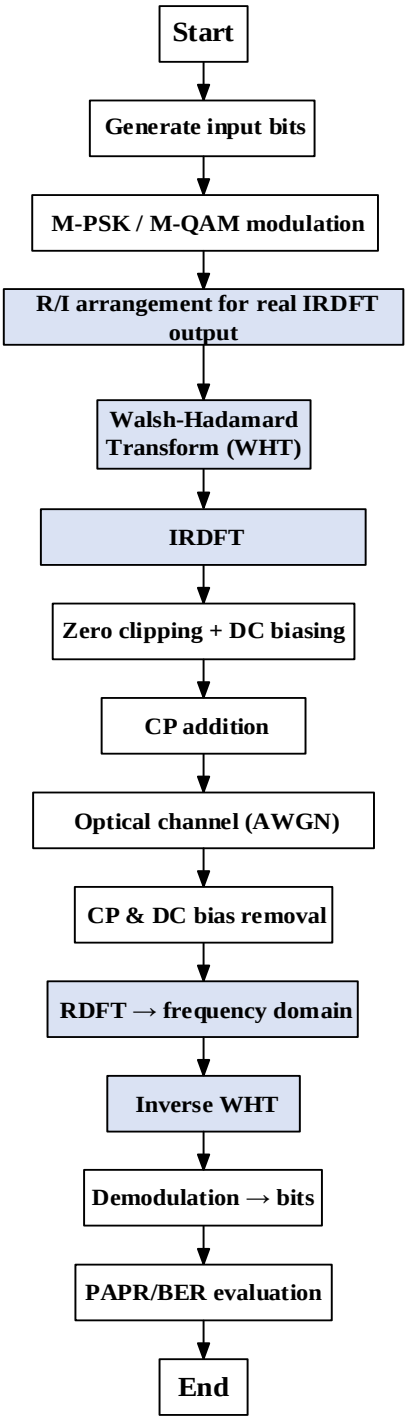

Figure 3. RDFT-WHT-based DCO-OFDM Flow Chart

The BER was evaluated by demodulating the received signals and comparing the reproduced bits with the original transmitted data as in Eq. (14):

$$BER = \frac{1}{N_b}\sum_{i=1}^{N_b}\{S(w) \neq S_D(w)\} \quad (14)$$

Where N_b is the total number of bits compared and calculated by Eq. (15):

$$N_b = symbols \times (\frac{N}{2} + 1) \times \log_2 M \tag{15}$$

The received signals were used to calculate PAPR along with CCDF plotting using Eq. 16

$$PAPR = \frac{\max\limits_{0 \le n < N+CP} |x_{CP}(n + CP)|^2}{\frac{1}{N + CP} \sum_{n=0}^{N+CP-1} |x_{CP}(n + CP)|^2} \tag{16}$$

This allows a comparison of PSK- and QAM-based RDFT schemes. Simulation results are presented for the DCO-OFDM-based and RDFT-WHT-based systems, both operating under the same conditions.

5. Results and discussion

The simulation results also showed that the performances for all the schemes RDFT matches DFT BER; WHT precoding does not change BER vs. RDFT. It is demonstrated that the proposed method, based on RDFT, performs well and can effectively resist AWGN. It can be observed from Fig. 4 that, under the same system configuration, the BER of the 16-PSK modulator is 10^{-4} at an SNR of approximately 33.5 dB for both the DFT- and RDFT-based systems. For the 16-QAM modulator in the same systems, a BER of 10^{-4} is obtained at an SNR of 29.5 dB. The RDFT and RDFT-WHT-based receivers share the same BER performance for 16-PSK, and they both achieve a BER of 10^{-4} at SNR ≈ 33.5 dB and ≃ 29.5 dB of a 16-QAM modulator at the same BER.

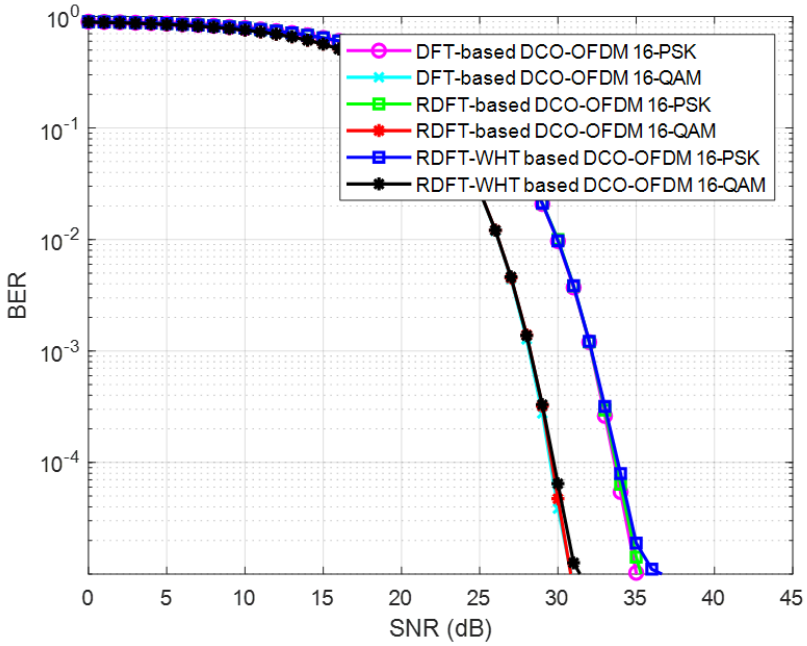

Figure 4. BER Performance for DFT, RDFT, and RDFT-WHT-Based DCO-OFDM Systems with 16-PSK and 16-QAM Modulators

The RDFT-WHT scheme outperforms the conventional RDFT in finding lower PAPR. The CCDF plots show that integration of WHT is beneficial to 16-PSK and 16-QAM DFT and RDFT, including 16-QAM modulation-based systems equally. Fig. 5 shows the PAPR performance of the two systems (RDFT and RDFT-WHT) working with the 16-PSK modulator. For RDFT-based and RDFT-WHT systems, the PAPR is approximately 9 dB and 8.5 dB, respectively, at a CCDF of 10^{-4}. For the 16-QAM-modulated RDFT-based system, the PAPR is approximately 9.1 dB (at a CCDF of 10^{-4}). The proposed RDFT-WHT system obtains around 8.8 dB at the same CCDF level. As M increases, it often signifies that the SNR required for a particular BER escalates, while the PAPR deteriorates slightly due to the increased density of the constellations. Reducing M produces the

contrary effect. For an equitable comparison, both families ought to be shown at M = 16. This method prevents modulation order effects from being confused with the effects of the transform/precoder.

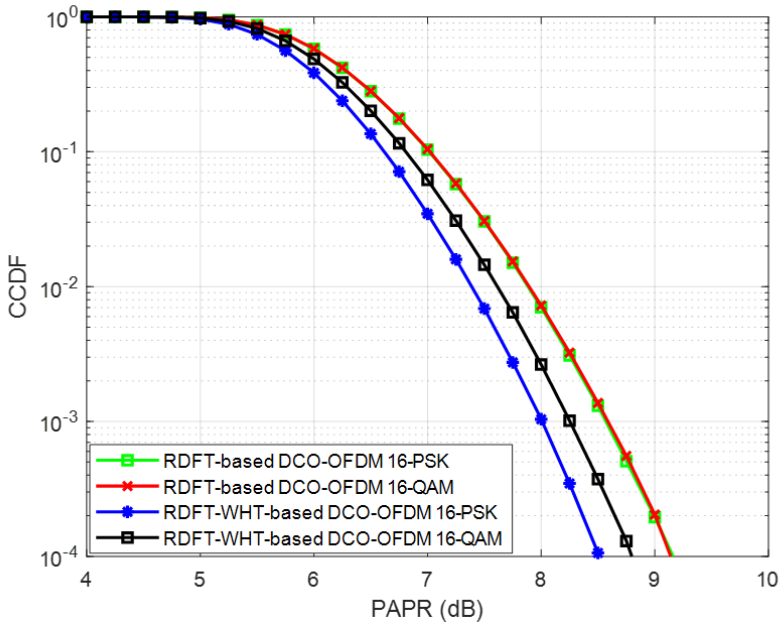

Figure 5. PAPR Performance for RDFT and RDFT-WHT-Based Systems with 16-PSK and 16-QAM Modulators

Figure 6 shows the number of multiplications for DFT and RDFT with various values of N utilizing Eq. (5) and Eq. (11), respectively. For $N = 1024$, the DFT requires 16,777,216 multiplications, while the RDFT needs only 8,388,608 multiplications.

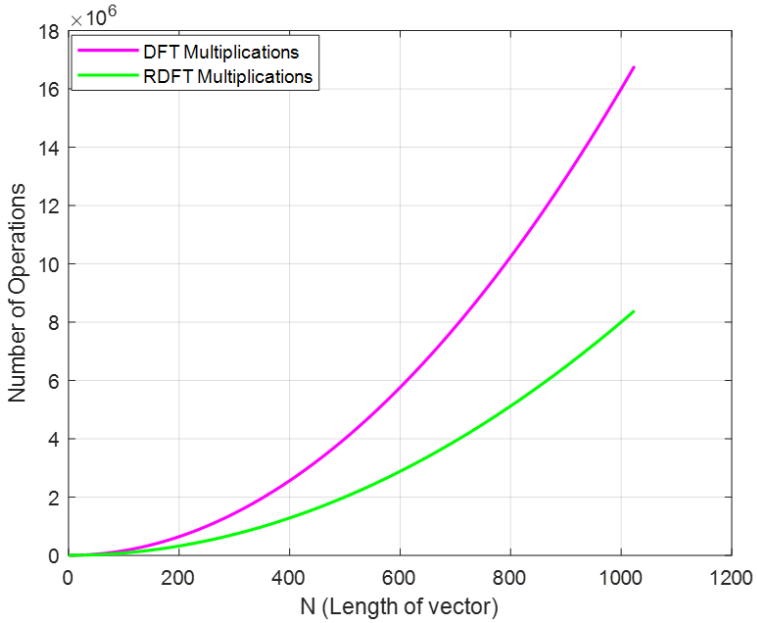

Figure 6. Comparison of The Number of Multiplications Between DFT and RDFT

From Eq. (6) and Eq. (12), the DFT needs 4,192,256 additions in Fig. 7, while the RDFT only requires 2,095,104. RDFT can speed up and optimize the operation of optical devices.

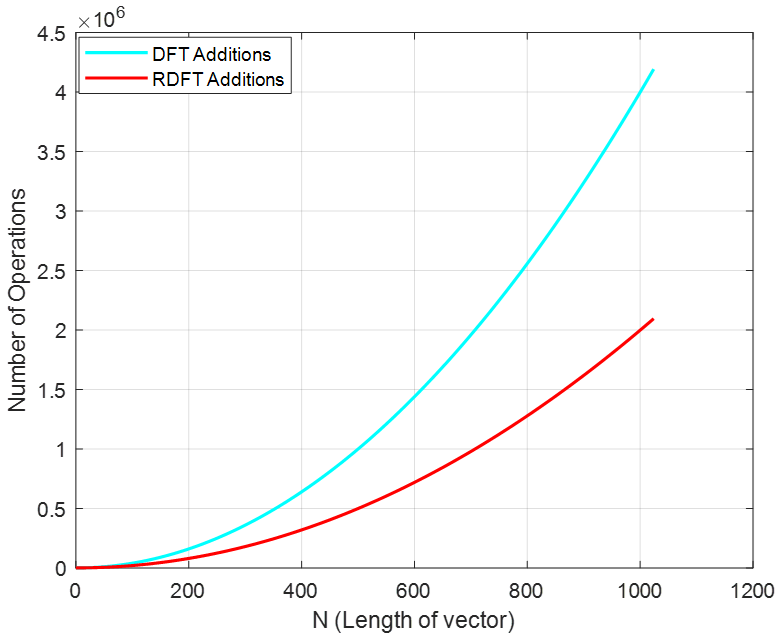

Figure 7. Comparison of The Number of Additions Between DFT and RDFT

6. Conclusion

This study evaluated a VLC DCO-OFDM system under three scenarios:

- Selection of transform (DFT versus RDFT),
- The activation or deactivation of WHT pre-coding,
- Constellation configuration (16-PSK versus 16-QAM), employing uniform parameters (AWGN, N = 256, $CP = N/4$, $BDC = 7$).

The key characteristic of RDFT is its ability to maintain the BER of standard DFT while reducing the number of mathematical operations by 50%. For N = 1024, the DFT requires 16,777,216 real multiplications and 4,192,256 additions, while the RDFT requires 8,388,608 multiplications and 2,095,104 additions. To achieve a BER of approximately 10^{-4}, 16-PSK requires an SNR of around 33.5 dB, while 16-QAM necessitates about 29.5 dB. The incorporation of WHT pre-coding results in a reduction of PAPR by approximately 0.3 to 0.5 dB at CCDF = 10^{-4}, exemplified by a decrease from 9.0 to 8.5 dB for 16-PSK and from 9.1 to 8.8 dB for 16-QAM, while maintaining BER levels. This facilitates compliance with LED/driver linearity standards and enhances power efficiency. Scenario trade-offs indicate that 16-QAM achieves the necessary BER with an SNR approximately 4 dB lower than that of 16-PSK, albeit with a marginally higher PAPR. PSK may be more suitable for applications that demand precise linearity. The system operates over an AWGN channel, free from indoor multipath and ambient interference. It excludes considerations for front-end nonlinearities or bias optimization, does not incorporate channel coding, synchronization, or MIMO, and permits only a single sweep of the N and M parameters. RDFT-WHT represents the optimal configuration due to its DFT-class BER, reduced PAPR, and significantly lower computational requirements for VLC links, enhancing both power and hardware efficiency.

Declaration of Competing Interest

The authors declare that there are no conflicts of interest regarding the publication of this manuscript.

Funding Information

No funding was received from any financial organization to conduct this research

Author Contributions

Ameen S. Jasim contributed to the conceptual design of the study, the implementation of both the conventional and modified systems, the development of simulations, and the preparation of the original manuscript draft. Mounir T. Hamood

provided supervision, guidance on methodological structure, critical manuscript revisions, and contributed to the final editing and review process. Both authors read and approved the final manuscript.

Acknowledgments

The authors express their gratitude to Wasit University, College of Engineering, Electrical Engineering Department in Al Kut, Wasit, Iraq, for supporting this study. In addition, I extend my gratitude to Mounir T. Hamood for his valuable advice on the academic writing of this paper.

References

[1] Y. A. Zenhom, E. K. I. Hamad, M. Alghassab, and M. M. Elnabawy, "Optical-OFDM VLC System: Peak-to-Average Power Ratio Enhancement and Performance Evaluation," *Sensors*, vol. 24, no. 10, p. 2965, 2024.

[2] S. M. Hameed, S. M. Abdulsatar, and A. A. Sabri, "BER Comparison and Enhancement of Different Optical OFDM for VLC," *International Journal of Intelligent Engineering and Systems*, vol. 14, no. 4, pp. 326–336, 2021.

[3] S. D. Dissanayake and J. Armstrong, "Comparison of ACO-OFDM, DCO-OFDM and ADO-OFDM in IM/DD systems," *Journal of Lightwave Technology*, vol. 31, no. 7, pp. 1063–1072, 2013.

[4] X. Y. Xu and D. W. Yue, "A Novel Non-Hermitian Symmetry Orthogonal Frequency Division Multiplexing System for Visible Light Communications," *IEEE Photonics Journal*, vol. 13, no. 6, pp. 1–9, 2021.

[5] R. Alindra, P. S. Priambodo, and K. Ramli, "Review of Orthogonal Frequency Division Multiplexing-Based Modulation Techniques for Light Fidelity," *Journal of Low Power Electronics and Applications*, vol. 13, no. 3, p. 46, 2023.

[6] S. Salih and M. Hamood, "Direct Algorithm for Computation of Inverse Real Fast Fourier Transform (IRDFT)," *Anbar Journal of Engineering Science*, vol. 14, no. 2, pp. 19–27, 2023.

[7] M. F. Sanya, L. Djogbe, A. Vianou, and C. Aupetit-Berthelemot, "DC-Biased Optical OFDM for IM/DD Passive Optical Network Systems," *Journal of Optical Communications and Networking*, vol. 7, no. 4, pp. 205–214, 2015.

[8] A. Ibrahim, T. Ismail, K. Elsayed, and M. S. Darweesh, "Odd Clipping Optical Orthogonal Frequency Division Multiplexing for VLC System," *International Journal of Communication Systems*, vol. 32, no. 16, p. e4150, 2019.

[9] D. Xin, Q. Xu, S. Qiao, and T. Zhang, "Non-Linear Companding Transform for DCO-OFDM-Based VLC Systems," *IET Communications*, vol. 13, no. 8, pp. 1110–1114, 2019.

[10] N. Boumaaz, H. Semlali, A. Maali, A. Soulmani, J. F. Diouris, and A. Ghammaz, "Low Complexity Spectrum Sensing Approach Applying Random Sampling in Cognitive Radio Networks," *IAENG International Journal of Computer Science*, vol. 49, no. 2, pp. 1–6, 2022.

[11] H. A. Leftah, "Efficient Optical OFDM System Resilience to Indoor Wireless Multipath Channels," *Iraqi Journal for Electrical and Electronic Engineering*, vol. 20, no. 1, pp. 78–83, 2024.

[12] R. G. Gallo, A. M. Abdelaziz, M. Alghoniemy, and H. M. Shalaby, "Real-DFT Based DCO-OFDM and ACO-OFDM for Optical Communications Systems," in *2019 21st International Conference on Transparent Optical Networks (ICTON)*, Angers, France, 2019: IEEE, pp. 1–4.

[13] J. Sospeter, E. Mwangi, and N. Mvungi, "Reduction of OFDM PAPR Using a Combined Hadamard Transformation and Selective Mapping for Terrestrial DAB+ System under Rayleigh and AWGN Channel," *Journal of Communications*, vol. 19, no. 6, pp. 266–273, 2024.

[14] N. Achebe, "Minimizing Peak to Average Power Ratio in OFDM System with WHT and Log Companding," *International Journal of Advanced Networking and Applications*, vol. 14, no. 2, pp. 5329–5333, 2022.

[15] Zenhom, Y.A., Hamad, E.K. and Elnabawy, M.M., 2024. Throughput improvement in ACO-OFDM-based VLC systems using noise cancellation and precoding techniques. *Optical and Quantum Electronics*, *56*(11), p.1798.